Original Russian Text © A. V. Artamonova, I. E. Kozlov, 2023,
published in MORSKOY GIDROFIZICHESKIY ZHURNAL, Vol. 39, Iss. 1 (2023)

Eddies in the Norwegian and Greenland Seas from the Spaceborne SAR Observations in Summer, 2007

A. V. Artamonova ✉, **I. E. Kozlov**

Marine Hydrophysical Institute of RAS, Sevastopol, Russian Federation
✉ *artamonovaocean@gmail.com*

Abstract

Purpose. The paper is aimed at analyzing the spatio-temporal variability of eddy field in the ice-free regions of the Norwegian and Greenland seas in summer, 2007 based on processing the spaceborne synthetic aperture radar (SAR) data, and its dependence on the background wind conditions and the surface current field.

Methods and Results. The Envisat ASAR radar images (RI) obtained in the *WSM* imaging mode with the 400 × 400 km swath width and the 150 × 150 m spatial resolution for May – October, 2007, were used as the initial data. The eddy surface manifestations were identified by an expert through the visual analysis of RI, after which the eddy diameter and rotation sign, as well as the total depth of the place corresponding to the eddy center, were determined. Information on the near-surface wind field was derived from the CMEMS WIND_GLO_PHY_CLIMATE_L4_REP_012_003 product based on the ASCAT scatterometer measurements carried out with the 0.25° spatial resolution. To analyze the relation between the eddy generation intensity and the surface currents' background field at the 1 m depth, the CMEMS GLORYS12V1 oceanic reanalysis with the 0.25° spatial resolution was applied. In total, more than 3000 surface eddy manifestations were recorded. The key regions where the eddies were observed and which were characterized by the eddies' maximum probability, were found over the Norwegian continental shelf east of the Vøring Plateau (water depth < 200 m), on the eastern slope of the Lofoten Basin, in the western part of the Denmark Strait and over the Iceland-Faroe Ridge. It is shown that the numbers of the observed cyclonic and anticyclonic eddies were equal. The observed eddies' diameters ranged within 0.5–150 km with the average value of ~ 14 km. Most often the eddies were observed over the depths not exceeding 500 m. The majority of eddy manifestations were identified under the northerly and northeasterly winds of 3–5 m/s and at the boundaries of currents whose velocities exceeded 0.3–0.4 m/s.

Conclusions. The number of cyclonic and anticyclonic eddies was recorded equal, which was comparable to the results of altimetry observations in the region, but differed from the results of SAR observations in the other Arctic and sub-Arctic regions where the cyclonic eddies dominated. The observed eddies were most often detected along the main jet currents and in the regions of their meandering.

Keywords: ocean eddies, radar images, SAR, Lofoten vortex, Norwegian Sea, Greenland Sea, GLORYS12V1, ASCAT

Acknowledgements: The study was carried out at financial support of the Russian Science Foundation grant No. 21-77-10052, https://rscf.ru/project/21-77-10052.

For citation: Artamonova, A.V. and Kozlov, I.E., 2023. Eddies in the Norwegian and Greenland Seas from the Spaceborne SAR Observations in Summer, 2007. *Physical Oceanography*, 30(1), pp. 112-123. doi:10.29039/1573-160X-2023-1-112-123

DOI: 10.22449/1573-160X-2023-1-112-123

Introduction

The Norwegian and Greenland seas are regions with high eddy activity, which plays an important role in the water redistribution between the Atlantic and Arctic oceans, as well as in the distribution of heat and nutrients [1–3].

The Lofoten Basin, located in the Norwegian Sea, is a transit reservoir. When the Atlantic waters pass through it, they deepen and transform, further falling into the Arctic basin. A distinctive feature of the region is the quasi-permanent anticyclonic Lofoten eddy, which is a lens of warm water with significant horizontal and vertical scales, located in the central part of the Lofoten Basin [4–6].

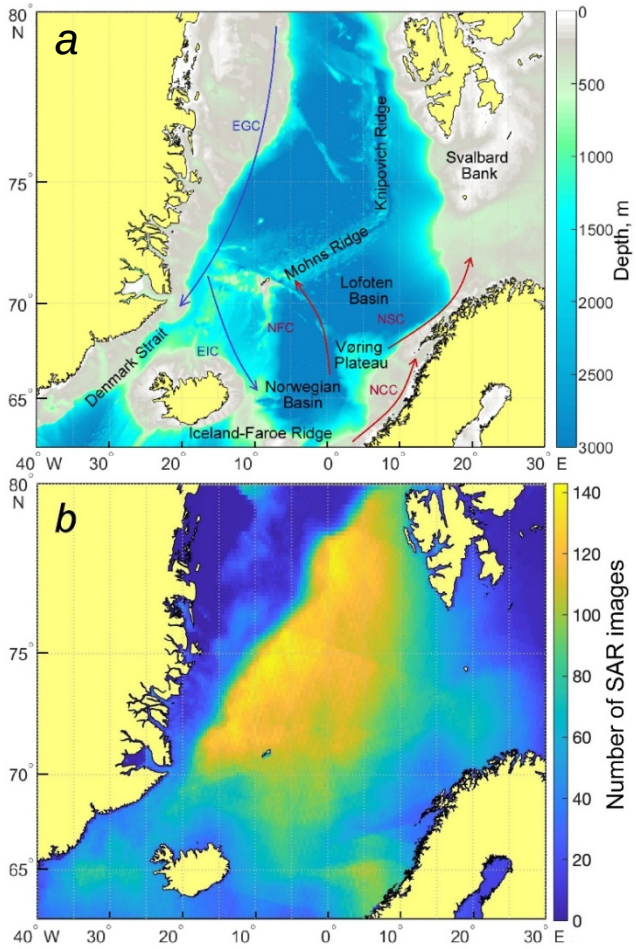

F i g. 1. Map of the study region including the GEBCO-based bathymetry and major geographical names. Arrows show the main currents: East Greenland (EGC), East Iceland (EIC), Norwegian Frontal (NFC), Norwegian slope (NSC) and Norwegian coastal (NCC) – *a*; coverage of the study region by the satellite SAR data, the number of available SAR images is shown in color – *b*

The water circulation in the study region (Fig. 1, *a*) is represented by the cold East Greenland current, which forms a branch of the East Iceland current in the Iceland region, and the warm Norwegian current, divided into the Norwegian frontal current, passing between the Norwegian and Lofoten basins, the Norwegian slope current moving north along the continental slope of Norway, and the Norwegian Coastal Current. A large number of large currents makes this region dynamically unstable, being an important factor for the generation of eddy structures. Based on the fact that eddies can transport a significant amount of heat

and other tracers over long distances [3], the study of their spatial distribution and characteristics is important, for example, to take into account in global and regional ocean circulation models.

The present paper is aimed at analyzing the spatio-temporal variability of eddy field in the ice-free regions of the Norwegian and Greenland seas in summer, 2007 based on processing the spaceborne synthetic aperture radar (SAR) data, and its dependence on the background wind conditions and the surface current field. A lot of works have been devoted to the study of eddy activity in the Norwegian and Greenland Seas, especially in the Lofoten Basin area, but most of them were based on satellite altimetry data [3, 5, 6–8]. Eddy studies based on the analysis of spaceborne SAR data were also carried out for this region [3, 8–10], but they considered only certain areas in the northern part of the Greenland Sea (Fram Strait) and in the Lofoten Basin, using completely different data arrays. In this paper, for the first time, the results of observations of eddy structures over such a vast area of the European sector of the Arctic are presented and the relationship between the spatiotemporal variability of the eddy field and the background fields of currents and surface wind, is analyzed, which determines the novelty of this research. The materials of the 6th International Scientific and Practical Conference were used in the paper [1].

Data and Methods

As is known, the generation and subsequent propagation of eddy structures are accompanied by changes in the field of surface currents and the formation of pronounced zones of convergence and divergence of currents with active modulation of wind ripples and films of surfactants. These factors lead to the formation of surface manifestations of eddy structures observed on spaceborne synthetic aperture radar (SAR) images of the sea surface in the form of backscatter contrasts of the radar signal [3, 11].

To analyze the eddy dynamics in the Norwegian and Greenland Sea waters, Envisat ASAR satellite radar images for May – October 2007 were used in the WSM survey mode with 400 × 400 km swath width and 150 × 150 m spatial resolution. In this analysis only the eddies observed on the ice-free sea surface areas were singled out.

Fig. 1b shows the spatial distribution of the number of analyzed SAR data for the study area, taking into account ice, i.e. after subtracting all radar image fragments with ice. The ice mask for each image was built on the basis of the Bremen University satellite product [12]. As can be seen, the largest amount of radar data (> 140) falls on the deep part of the Greenland Sea, including the Fram Strait, as well as on the area near the Vøring Plateau in the Norwegian Sea (~ 100). The minimum amount of radar data falls on the shelf areas of the Greenland Sea, where ice cover is observed throughout almost the entire summer season.

[1] Artamonova, A. and Kozlov, I., 2021. Characteristics of Ocean Eddies in the Norwegian and Greenland Seas from Spaceborne Radar Observations in 2007. In: MSTU, 2021. *Fundamental and Applied Aspects of Geology, Geophysics and Geoecology Using Modern Information Technologies. Materials of the 6th International Scientific and Practical Conference*. Maykop: IP Kucherenko V.O. Publ. Part 1, pp. 25-30 (in Russian).

Based on the analysis of the surface manifestations of eddies in SAR images (Fig. 2), the regions of eddy generation, their diameter, sign of rotation and depth corresponding to the eddy center were found. Characteristics of eddy structures were determined based on the technique described in [13]. Data analysis and processing of results were carried out in *Mathworks ©MatLab*. After the visual identification of the surface manifestations of eddies, the expert determined various characteristics of the them.

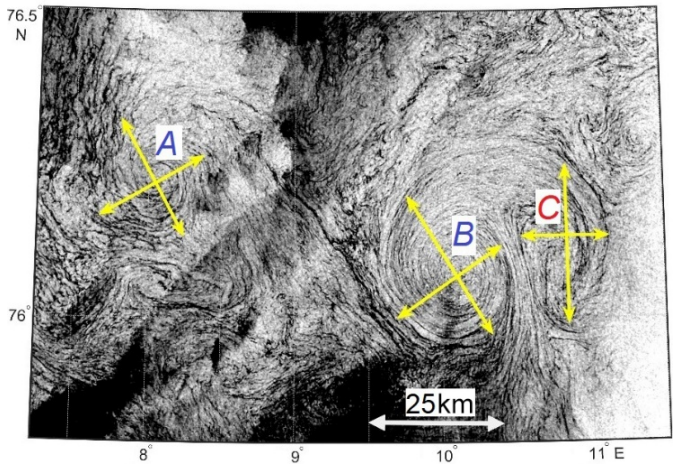

F i g. 2. Examples of eddy manifestations on the Envisat ASAR image (July 25, 2007) conditioned by the accumulation of surface films in the surface currents convergence zones. Yellow arrows mark the diameters of the cyclonic (*A*, *B*) and anticyclonic (*C*) eddies

As already mentioned, eddy structures in SAR images are observed due to a change in the sea surface roughness, which in turn depends on the interaction of the fields of currents and wind with surface films and waves. The most favorable factors for observing open water eddies on radar images are weak and moderate winds [2] [14, 15].

To obtain wind data, the CMEMS WIND_GLO_PHY_CLIMATE_L4_REP_012_003 product, based on ASCAT scatterometer data with a spatial resolution of 0.25°, was used.

To analyze the relationship between the intensity of eddy generation and background current fields, the CMEMS GLORYS12V1 oceanic reanalysis with a spatial resolution of 0.25° at a horizon of 1 m, was used. This reanalysis well reproduces the main characteristics of the current fields, as well as their mesoscale variability [6].

Results

In total in the course of the work, 730 Envisat ASAR radar images for May – October 2007 were analyzed, in which 3327 surface manifestations of eddies were identified. It can be seen (Fig. 3) that the difference in the distribution of the total

[2] Dokken, S.T. and Wahl, T., 1996. *Observations of Spiral Eddies along the Norwegian Coast in ERS SAR Images.* Kjeller, Norge: Norwegian Defence Research Establishment, 29 p.

number of radar images by months is insignificant. At the same time, the largest number of surface manifestations of eddies was registered in May (1121), the smallest – in October (47).

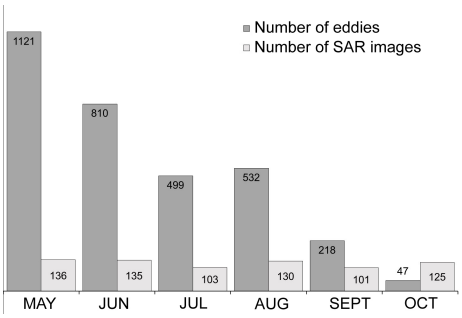

F i g. 3. Histograms of distribution of the number of radar images and the recorded eddies in May – October, 2007

Fig. 4 shows the spatial distribution of all eddies identified. There were 1627 anticyclones and 1600 cyclones identified, which significantly differs from the results obtained earlier for other Arctic seas [3, 9, 11, 13, 16]. The largest accumulations of eddies were found in the Vøring Plateau region, on the Norwegian frontal current periphery, on the eastern slope of the Lofoten Basin, similarly to the results of [3], along the Mon and Knipovich ridges, in the Danish Strait and over the Faroe-Iceland threshold. This location is most likely owing to the meandering of the East Greenland and Norwegian currents due to their baroclinic and barotropic instability, the interaction of these currents with the Lofoten eddy, and significant topographical inhomogeneities (ridges, basins), where eddy structures are most common.

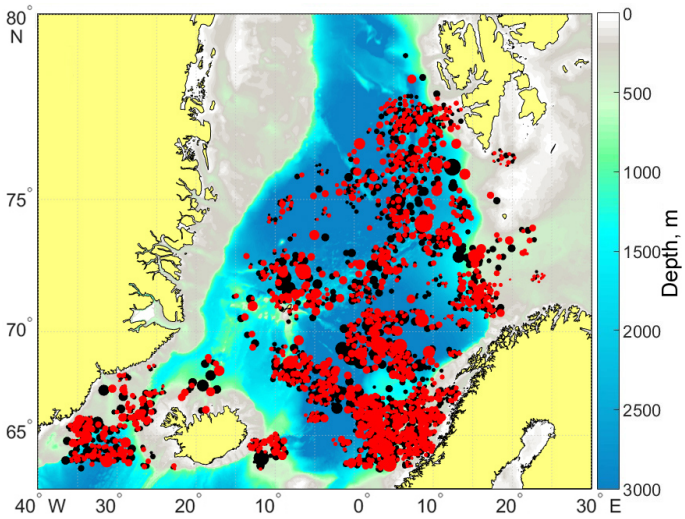

F i g. 4. Spatial distribution of the eddies identified in the SAR data in May – October, 2007. Black (red) circles indicate the cyclonic (anticyclonic) eddies. The marker size is proportional to the eddy diameters

The histogram of the distribution of the registered eddy diameters is shown in Fig. 5, *a*. The diameters of the observed eddies generally did not exceed 15 km (2260 out of 3327 eddies). The average recorded diameter was 13.9 km. The average diameter of anticyclonic and cyclonic eddies differs slightly (13.98 and 13.85 km, respectively). The maximum recorded diameter was 154 km; no significant differences were found for cyclones and anticyclones in this parameter.

In [9, 17] it was shown that in the range of eddy diameters ~ 15–30 km, the difference in the ratio between cyclones and anticyclones decreases, and at large diameters, anticyclonic eddies begin to dominate. According to the results of the present paper, the number of cyclonic and anticyclonic eddy structures up to 15 km in diameter is also approximately the same (1119 and 1133, respectively).

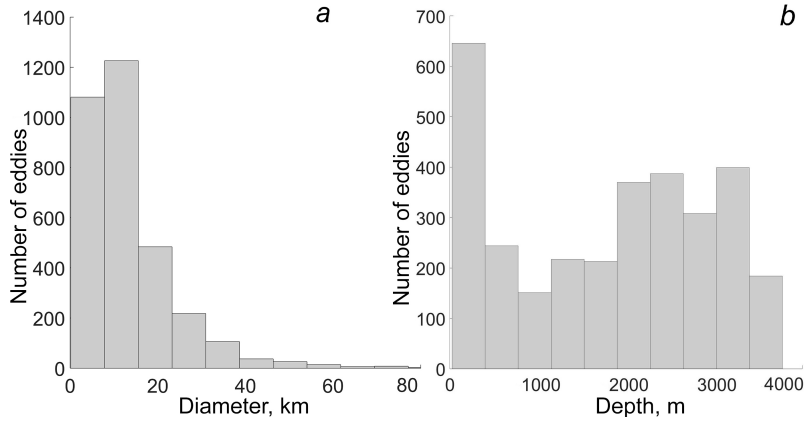

F i g. 5. Histograms of distribution of the eddy diameters – *a* and depths over which the eddies were identified – *b*

The histogram of the depth distribution over which the eddies were recorded is shown in Fig. 5, *b*. Eddies were observed at depths of 26–3776 m. Their greatest number was recorded above depths not exceeding 500 m, however, a significant number were also located above deep-water areas with depths > 1000 m.

Fig. 6a shows the spatial distribution of the total number of identified eddies on a grid of 50 × 50 cells (the cell area is 3.05 km^2 on average). The largest number of eddies was found in the same areas as noted above. Fig. 6b shows the spatial distribution of the frequency of eddy observations in the study area, obtained as the ratio of the total number of eddies at a grid node to the number of SAR observations of this node. This normalized characteristic allows the most accurate identification of key areas of intense eddy formation. As can be seen, the maximum frequency of eddy observations (0.4 and higher) was recorded on the Norwegian shelf east of the Vøring Plateau with depths of no more than 200 m, on the eastern slope of the Lofoten Basin, in the western part of the Denmark Strait, over the Faroe – Iceland threshold and on the Greenland shelf Danish Strait with depths less than 200 m.

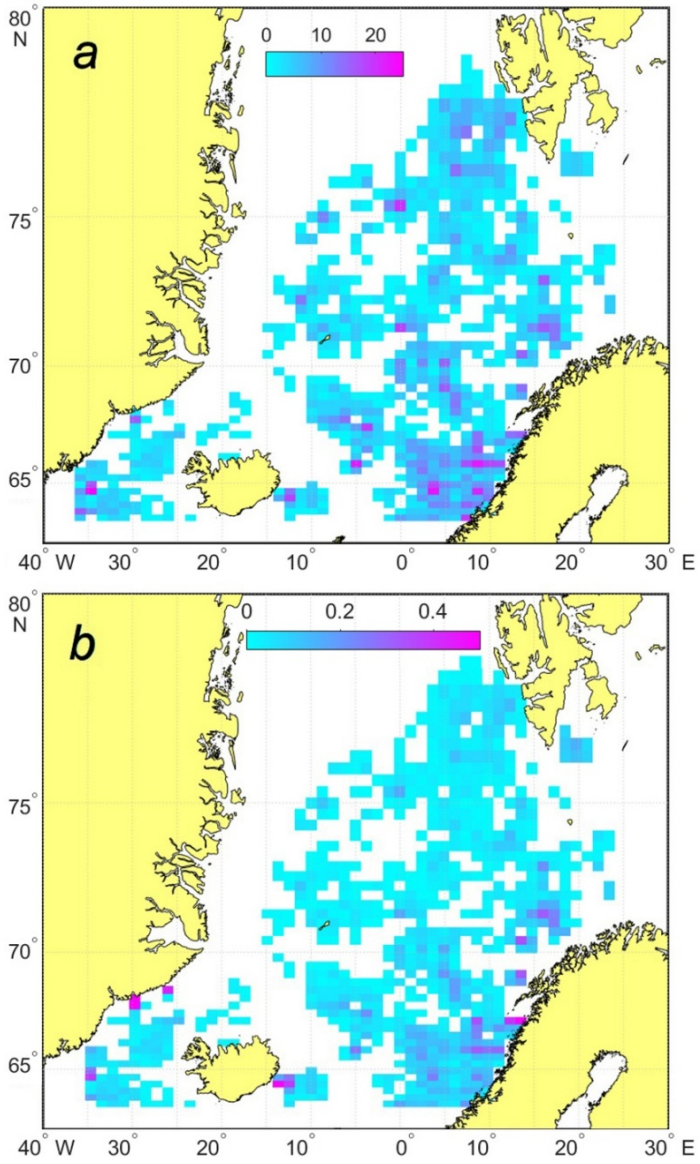

F i g. 6. Spatial distribution per a grid square of: *a* – total number of the eddies identified using the satellite SAR data in May – October, 2007; *b* – probability of eddy observations

Fig. 7 shows the spatial distribution of the average (Fig. 7, *a*) and maximum (Fig. 7, *b*) eddy diameters on a grid of 50 × 50 cells. These distributions are generally similar. Eddies with the largest average (50 km or more) and maximum (100 km or more) diameters were recorded in the area of the Mona and Knipovich ridges, on the eastern slope of the Lofoten Basin, and also on the Norwegian frontal current periphery.

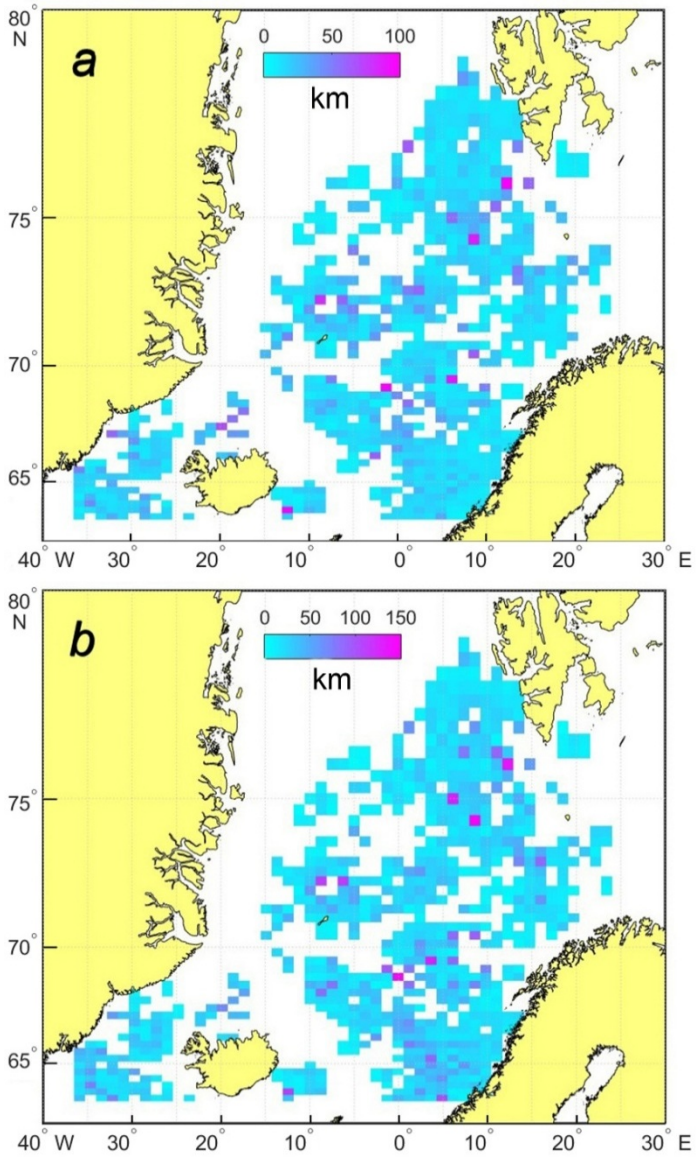

F i g. 7. Spatial distribution of the average (*a*) and maximum (*b*) diameters of the eddies identified by the SAR data in May – October, 2007

To analyze the relationship between the eddy generation intensity and the background fields of surface currents and wind, Fig. 8 shows the average monthly spatial distributions of eddy frequency (left), current velocity and direction (center), wind speed and direction (right) in May – August 2007.

Overall, returning to Fig. 4, we can say that the eddies are mainly located on the periphery of the jets of the main currents with velocities ranging 0.1–0.4 m/s, and in some cases even exceeding these values. In all months, the quasi-stationary anticyclonic Lofoten eddy is clearly visible in the field of currents, on the periphery of which a large number of smaller eddies were found in the SAR data (Fig. 7).

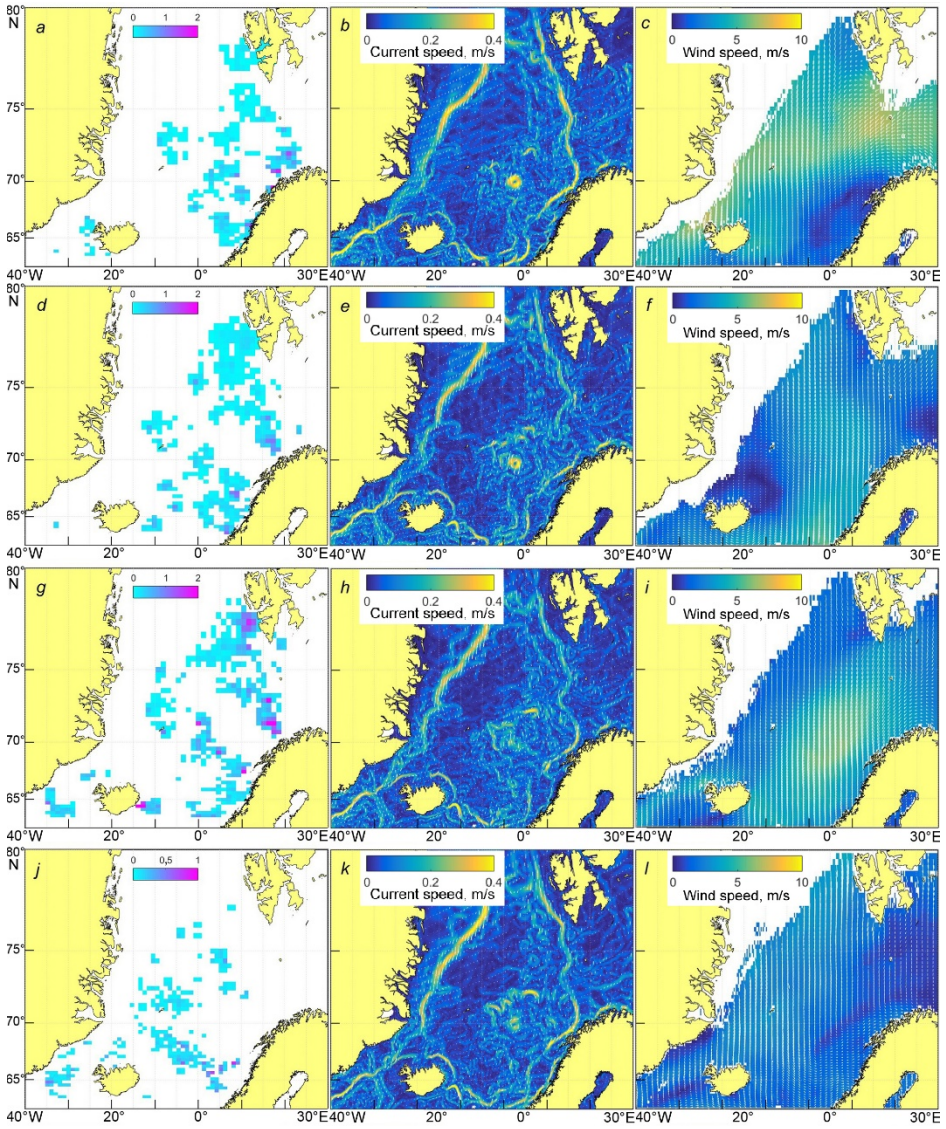

F i g. 8. Spatial distribution of: monthly averages of eddy observation probability per a grid square of 50 × 50 cells (left), surface current velocities (middle) and near-surface wind speed (right) in May – August, 2007

In May (Fig. 8, *a* – *c*), when the largest number of eddies was recorded over the entire period, the maximum intensity of the main currents over this period was also observed. Thus, for the jets of the Norwegian, East Greenland and East Iceland currents, the maximum velocities reached over 0.3–0.4 m/s. It is interesting to note that ice cover was still observed in the area of the East Greenland Current in May. Despite the intensity of this current, open water eddies were not observed near it, while eddies in the marginal ice zone were noted regularly [16]. In general, this month, the northeast wind dominated with average speeds of ~ 3–4 m/s.

In June (Fig. 8, *d* – *f*), eddies were more common in places where the Norwegian Current branches were meandering, as well as in the area of its collision with the East Iceland Current. In places of intense generation of eddies, the wind of the northern and northeastern directions was observed with speeds of 3–5 m/s.

In July (Fig. 8, *g* – *i*), the main sources of eddy generation actually completely coincided with those in June and were located in the areas of change of direction and intensification of the Norwegian Current branches, to the southwest of Svalbard on the warm stream of the West Spitsbergen current and on the periphery of the Lofoten eddy. The wind conditions in the places of the greatest accumulation of eddy structures were characterized by a northeastern wind with speeds of 3–5 m/s.

In August (Fig. 8, *j* – *l*), eddies were more common on the Lofoten eddy periphery and in places of the East Greenland Current intensification and meandering in the Denmark Strait. August is distinguished by low wind speeds up to 4 m/s, predominantly northern.

The results for September and October are not presented due to the significantly smaller number of eddy structures identified. The intensity of the main currents in these months was slightly less. But the main reason for the rarer registration of eddy structures, apparently, was the higher average values of near-surface wind speed, up to 8 m/s, which limit the reliable identification of eddies in spaceborne SAR data. In the areas where eddies were observed, the average wind speed was lower and did not exceed 5 m/s.

Conclusions

A distinctive feature of the surface manifestations of eddies in the study area for May – October 2007 is approximately the same number of identified cyclonic and anticyclonic eddies, which is similar to the results of altimetry observations in this area. This result differs substantially from the results obtained in similar studies for other Arctic seas, where cyclones usually significantly prevailed over anticyclones. Presumably, this is due to the size of the observed eddies. In the present case, the average diameter of the observed eddies was ~ 15 km, which is 2–3 times higher than the average sizes of eddies in other Arctic seas and is largely determined by the Rossby deformation radius.

It is shown that the most intense areas of eddy formation are those near the Vøring Plateau, in the Danish Strait, above the Faroe – Iceland threshold, on the quasi-stationary Lofoten eddy periphery and along the Norwegian Current branches. A large number of eddies were also observed in the region of the Mona and Knipovich ridges, along the main jet of the West Spitsbergen Current in the Fram Strait and on the western shelf of Svalbard.

The maximum number of eddies was observed along the jets of the main currents, especially in their meandering areas. The largest number of eddies was recorded in May, when the intensity of the main currents was at its maximum. The decrease in the number of identified eddies in September – October 2007 is explained by higher near-water wind speeds relative to summer months, which limit the registration of surface manifestations of eddies in satellite data.

The most favorable factors, under which a significant number of eddy structures were recorded, were northern and northeastern winds with a speed ranging 3–5 m/s.

REFERENCES

1. Kamenkovich, V.M., Koshlyakov, M.N. and Monin, A.S., eds., 1986. *Synoptic Eddies in the Ocean*. Dordrecht: Springer, 444 p. https://doi.org/10.1007/978-94-009-4502-9
2. Hansen, C., Kvaleberg, E. and Samuelsen, A., 2010. Anticyclonic Eddies in the Norwegian Sea; Their Generation, Evolution and Impact on Primary Production. *Deep Sea Research Part I: Oceanographic Research Papers*, 57(9), pp. 1079-1091. doi:10.1016/j.dsr.2010.05.013
3. Bashmachnikov, I.L., Kozlov, I.E., Petrenko, L.A., Glock, N.I. and Wekerle C., 2020. Eddies in the North Greenland Sea and Fram Strait from Satellite Altimetry, SAR and High-Resolution Model Data. *Journal of Geophysical Research: Oceans*, 125(7), e2019JC015832. doi:10.1029/2019JC015832
4. Novoselova, E.V. and Belonenko, T.V., 2020. Isopycnal Advection in the Lofoten Basin of the Norwegian Sea. *Fundamental and Applied Hydrophysics*, 13(3), pp. 56-67. doi:10.7868/S2073667320030041 (in Russian).
5. Travkin, V.S. and Belonenko, T.V., 2019. Seasonal Variability of Mesoscale Eddies of the Lofoten Basin Using Satellite and Model Data. *Russian Journal of Earth Sciences*, 19(5), ES5004. doi:10.2205/2019ES000676
6. Zinchenko, V.A., Gordeeva, S.M., Sobko, Yu.V. and Belonenko, T.V., 2019. Analysis of Mesoscale Eddies in the Lofoten Basin Based on Satellite Altimetry. *Fundamental and Applied Hydrophysics*, 12(3), pp. 46-54. doi:10.7868/S2073667319030067
7. Raj, R.P., Halo, I., Chatterjee, S., Belonenko, T., Bakhoday-Paskyabi, M., Bashmachnikov, I., Fedorov, A. and Xie, J., 2020. Interaction between Mesoscale Eddies and the Gyre Circulation in the Lofoten Basin. *Journal of Geophysical Research: Oceans*, 125(7), e2020JC016102. doi:10.1029/2020JC016102
8. Zimin, A.V. and Atadzhanova, O.A., 2020. Estimation of the Characteristics of Mesoscale Eddies in the Basin of the Lofoten Depression from Satellite and Ship Observations. *Sovremennye Problemy Distantsionnogo Zondirovaniya Zemli iz Kosmosa*, 17(3), pp. 202-210. doi:10.21046/2070-7401-2020-17-3-202-210 (in Russian).
9. Kozlov, I.E. and Atadzhanova, O.A., 2022. Eddies in the Marginal Ice Zone of Fram Strait and Svalbard from Spaceborne SAR Observations in Winter. *Remote Sensing*, 14(1), 134. https://doi.org/10.3390/rs14010134
10. Petrenko, L.A. and Kozlov, I.E., 2020. Properties of Eddies near Svalbard and in Fram Strait from Spaceborne SAR Observations in Summer. *Sovremennye Problemy Distantsionnogo Zondirovaniya Zemli iz Kosmosa*, 17(7), pp. 167-177. doi:10.21046/2070-7401-2020-17-7-167-177 (in Russian).
11. Artamonova, A.V., Kozlov, I.E. and Zimin, A.V., 2020. Characteristics of Ocean Eddies in the Beaufort and Chukchi Seas from Spaceborne Radar Observations. *Sovremennye Problemy Distantsionnogo Zondirovaniya Zemli iz Kosmosa*, 17(1), pp. 203-210. doi:10.21046/2070-7401-2020-17-1-203-210 (in Russian).
12. Spreen, G., Kaleschke, L. and Heygster, G., 2008. Sea Ice Remote Sensing Using AMSR-E 89-GHz Channels. *Journal of Geophysical Research: Oceans*, 113(C2), C02S03. doi:10.1029/2005JC003384
13. Kozlov, I.E., Artamonova, A.V., Manucharyan, G.E. and Kubryakov A.A., 2019. Eddies in the Western Arctic Ocean from Spaceborne SAR Observations over Open Ocean and Marginal Ice Zones. *Journal of Geophysical Research: Oceans*, 124(9), pp. 6601-6616. doi:10.1029/2019JC015113

14. Karimova, S., 2012. Spiral Eddies in the Baltic, Black and Caspian Seas as Seen by Satellite Radar Data. *Advances in Space Research,* 50(8), pp. 1107-1124. doi:10.1016/j.asr.2011.10.027

15. Shuchman, R.A., Burns, B.A., Johannessen, O.M., Josberger, E.G., Campbell, W.J., Manley, T.O. and Lannelongue, N., 1987. Remote Sensing of the Fram Strait Marginal Ice Zone. *Science*, 236(4800), pp. 429-431. doi:10.1126/science.236.4800.429

16. Atadzhanova, O.A., Zimin, A.V., Romanenkov, D.A. and Kozlov, I.E., 2017. Satellite Radar Observations of Small Eddies in the White, Barents and Kara Seas. *Physical Oceanography*, (2), pp. 75-83. doi:10.22449/1573-160X-2017-2-75-83

17. Karimova, S., 2017. Observations of Asymmetric Turbulent Stirring in Inner and Marginal Seas Using Satellite Imagery. *International Journal of Remote Sensing*, 38(6), pp. 1642-1664. doi:10.1080/01431161.2017.1285078

About the authors:

Anastasia V. Artamonova, Junior Research Associate, Marine Hydrophysical Institute of RAS (2 Kapitanskaya Str., Sevastopol, 299011, Russian Federation), **WoS ResearcherID: AAD-2817-2022**, **Scopus Author ID: 57210964315**, **ORCID ID: 0000-0002-1154-3372**, **SPIN-code: 1478-6492 AuthorID: 965452**, artamonovaocean@gmail.com

Igor E. Kozlov, Leading Research Associate, Head of Marine Polar Research Laboratory, Marine Hydrophysical Institute of RAS (2 Kapitanskaya Str., Sevastopol, 299011, Russian Federation), Ph.D (Phys.-Math), **ORCID ID: 0000-0001-6378-8956**, **ResearcherID: G-1103-2014**, **Scopus Author ID: 49963767500**, ik@mhi-ras.ru

Contribution of the co-authors:

Anastasia V. Artamonova – data collection and systematization; data analysis; methodology; data visualization, selection and analysis of literature; writing the original text of the article; review and editing

Igor E. Kozlov – conceptualization; methodology; software; selection and analysis of literature; review and editing; project administration; funding acquisition

The authors have read and approved the final manuscript.
The authors declare that they have no conflict of interest.